



ORIGINAL ARTICLE

Novel coumarin derivatives as potential tyrosinase inhibitors: Synthesis, binding analysis and biological evaluation



Li Lu^{a,1}, Xin Zhang^{a,1}, Yu Kang^a, Zhuang Xiong^a, Kun Zhang^a, Xuetao Xu^{a,*}, Liping Bai^{b,*}, Hongguang Li^{a,*}

^a School of Biotechnology and Health Sciences, Wuyi University, Jiangmen 529020, PR China

^b State Key Laboratory of Quality Research in Chinese Medicine, Macau Institute for Applied Research in Medicine and Health, Guang dong-Hong Kong-Macao Joint Laboratory of Respiratory Infectious Disease, Macau University of Science and Technology, Macau 999078, PR China

Received 1 November 2022; accepted 22 February 2023

Available online 27 February 2023

KEYWORDS

Tyrosinase;
Melanogenesis;
Coumarin;
Cinnamic acid

Abstract A novel series of thirty coumarin derivatives (**4a** ~ **r**, **5a** ~ **l**) constituted by coumarin and cinnamic acid/benzoic acid through oxime linkage were synthesized and evaluated for their potential anti-tyrosinase activity. Among them, compound **5l** exhibited outstanding anti-tyrosinase activity with IC₅₀ of 3.04 ± 0.01 μM compared to 14.13 ± 0.80 μM of kojic acid. Kinetic study revealed compound **5l** to be a reversible and uncompetitive tyrosinase inhibitor. 3D fluorescence and CD spectra results showed treatment of compound **5l** lead to the conformational changes of tyrosinase. Molecular docking revealed the binding between compound **5l** and tyrosinase. Furthermore, compound **5l** inhibited melanin content and cellular tyrosinase activity both in B16F10 cells and zebrafish model with no toxicity effect. Taken together, our findings suggested that compound **5l** could be used as potential candidate to relieve tyrosinase-related hyperpigmentation.

© 2023 The Author(s). Published by Elsevier B.V. on behalf of King Saud University. This is an open access article under the CC BY-NC-ND license (<http://creativecommons.org/licenses/by-nc-nd/4.0/>).

1. Introduction

Melanin, produced by melanocytes, is widely distributed in humans, animals, and plants (Lin and Fisher, 2007). It is a vital biological pigment responsible for skin, hair, and eye color of humans (Moreiras et al., 2020). The production of melanin leads to the pigmentation that protects the skin against from ultraviolet related injuries (Pillaiyar

et al., 2018). However, excess accumulation of melanin characterizes multiplex hyperpigmentary disorders, including melasma, freckles, and melanoma (Roberts et al., 2015). Melanogenesis is a complex process involving series of chemical and enzymatic reactions (Imokawa et al., 2015).

Tyrosinase as the only rate-limiting enzyme in melanogenesis, is crucial for melanogenesis in human skin cells (Zolghadri et al., 2019). Tyrosinase is responsible for the first two catalytic steps in biosynthetic process of melanin: hydroxylation reaction of tyrosine to L-dihydroxyphenylalanine (L-DOPA) and subsequent oxidation reaction of L-DOPA to dopaquinone (Parvez et al., 2007). Immediately, dopaquinone was catalytic converted to melanin by

* Corresponding authors.

E-mail addresses: xuetaoxu@wyu.edu.cn (X. Xu), lpbai@must.edu.mo (L. Bai), wyuchemlhg@126.com (H. Li).

¹ Li Lu and Xin Zhang contributed equally to this work.

tyrosinase-related proteins (Sánchez-Ferrer et al., 1995). Thence, the regulation of tyrosinase activity is vital for the prevention of melanin synthesis (Yuan et al., 2020). To date, a huge number of natural and synthetic tyrosinase inhibitors have been developed (Li et al., 2021; Fu et al., 2021; Ashooriha et al., 2020). However, only a few inhibitors including arbutin and kojic acid are used as marketable therapeutic agents. But they still present the undesirable side-effects, including dermatitis, cytotoxicity, and skin cancer. These problems prompt us to discover safer and more active tyrosinase inhibitors.

Coumarin, an important core skeleton existing in natural products, presents various pharmacological activities, such as anti-oxidation, anti-inflammatory, anti-bacterial, and anti-cancer (Xu et al., 2020; Kostova, 2005; Musa and Cooperwood, 2008). Importantly, lots of coumarin derivatives presented potential inhibition on tyrosinase or/and melanin (Ashraf et al., 2015; Matos et al., 2015; Asthana et al., 2015). Liu et al. (Liu et al., 2012) reported the synthesis of coumarin esters with the most potent tyrosinase inhibition $IC_{50} = 3.4 \mu\text{M}$ (Fig. 1). Matos et al. (Matos et al., 2011) developed halogenated phenylcoumarins as tyrosinase inhibitors (most potent tyrosinase inhibition $IC_{50} = 0.25 \mu\text{M}$) (Fig. 1). Pang et al. (Pang et al., 2017) synthesized novel isoxazole contained coumarin derivatives that showed better activity on melanin synthesis than positive control 8-methoxypsoralen (Fig. 1). On the other hand, cinnamic acid/benzoic acid, active ingredients widely found in natural plants, have been recognized as the privileged scaffolds in the drug research and development due to their broad-spectrum pharmacological activities (Jitareanu et al., 2013; Xu et al., 2005; Taofiq et al., 2017). Especially, cinnamic acid/benzoic acid, and their derivatives have been reported to exhibit anti-tyrosinase or/and anti-melanin ability effects (Kong et al., 2008; Sheng et al., 2018; Ullah et al., 2018). Romagnoli et al. (Romagnoli et al., 2022) reported arylpiperazine linked cinnamic acid derivatives presenting good inhibitory against tyrosinase activity and melanin synthesis (Fig. 1). Cinnamide derivatives also showed excellent inhibitory activity toward tyrosinase and melanin (Fig. 1) (Ullah et al., 2019). Benzoic acid-thymol ester (Ashraf et al.) demonstrated good anti-tyrosinase activity (Ashraf et al., 2015). In addition,

the oxime core prevalently exists in lots of anti-tyrosinase active compounds, including chalcone oximes (Radhakrishnan et al., 2016), and hydroxypyridinone oxime ether derivatives (Shao et al., 2018) (Fig. 1).

Molecular hybridization has been recognized as an important structural modification strategy to design new drugs, that combine two or more pharmacophoric moieties to yield a new hybrid molecule. As part of our ongoing efforts to develop safer and more active tyrosinase inhibitors, the hybrids of coumarin with cinnamic acid/benzoic acid through oxime linkage (Fig. 1) were designed and synthesized. Then the synthetic derivatives were assayed for their anti-tyrosinase activity, followed by the investigation of B16F10 cell-based and zebrafish-based experiments.

2. Results and discussion

2.1. Chemistry

All coumarin-cinnamic acid/benzoic acid derivatives (**4a** ~ **r**, **5a** ~ **l**) were synthesized as synthetic route in Scheme 1. Substituted salicylaldehyde (**1**) reacted with ethyl acetaacetate to produce substituted acetyl coumarin (**2**), followed by the reaction with hydroxylamine hydrochloride to obtain substituted coumarin containing oxime (**3**). Finally, coumarin containing oxime underwent esterification with substituted cinnamic acid/benzoic acid chloride to yield target compounds. All synthetic derivatives (**4a** ~ **r**, **5a** ~ **l**) were identified by ^1H NMR, ^{13}C NMR and HRMS.

2.2. Anti-tyrosinase activity and SAR analysis

For finding more active tyrosinase inhibitors, coumarin-cinnamic acid derivatives (**4a** ~ **i**) and coumarin-benzoic acid derivatives (**4j** ~ **r**) were firstly synthesized. Due to the solubil-

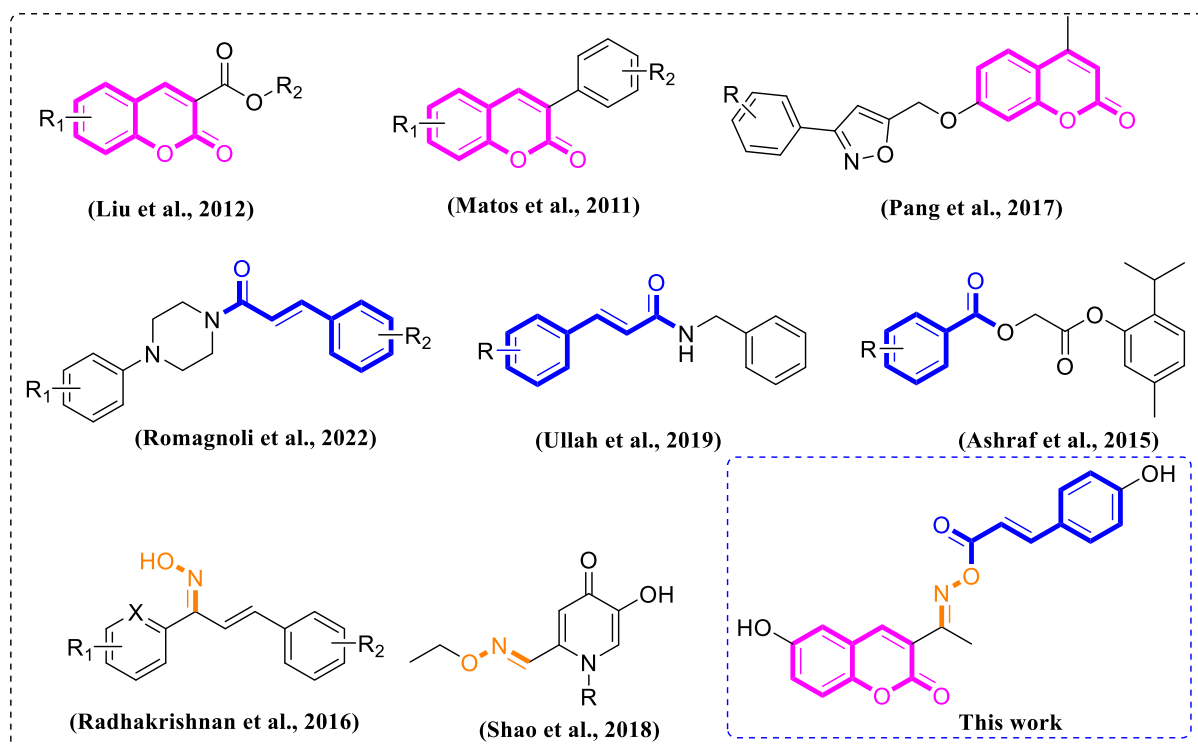
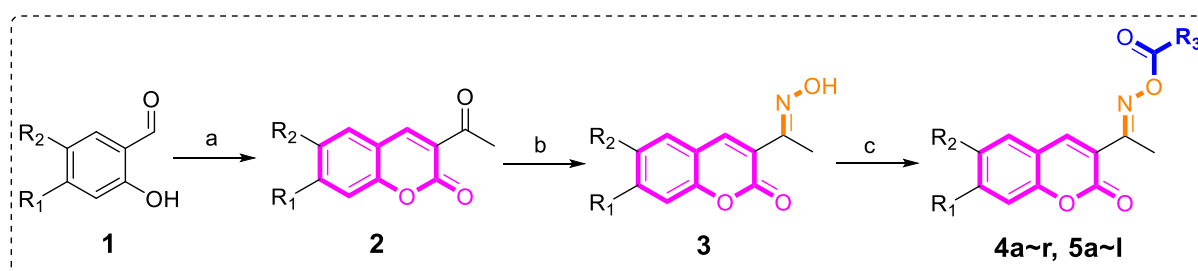


Fig. 1 Rationale of the current study.



Scheme 1 Synthesis of coumarin-cinnamic acid/benzoic acid derivatives **4a** ~ **r** and **5a** ~ **l**. Reagents and condition: (a) Ethyl acetaacetate, Piperidine, EtOH, 80 °C; (b) Hydroxylamine hydrochloride, Pyridine, EtOH, rt; (c) Substituted benzoic acid chloride/cinnamic acid chloride, triethylamine, DCM, rt.

ities of some coumarin derivatives at enzyme activity test system were not good enough, $\sim 64 \mu\text{M}$. For better comparing the inhibition activity of coumarin derivatives and future structure–activity relationship analysis, we firstly tested the anti-tyrosinase activity of compounds at concentration of $64 \mu\text{M}$ using kojic acid as positive control. As depicted in Table 1, among 18 derivatives, compound **4i** with 4-hydroxyl group in benzene ring of cinnamic acid exerted strongest tyrosinase inhibition ($61.24 \pm 0.17\%$) at concentration of $64 \mu\text{M}$, while other derivatives showed weaker inhibition against tyrosinase activity ($< 50\%$). Interesting, compound **4i** (IC_{50} : $6.40 \pm 0.39 \mu\text{M}$) presented about ~ 2.2 folds stronger tyrosinase inhibitory effect than kojic acid ($14.13 \pm 0.80 \mu\text{M}$).

The main differences between derivatives **4a** ~ **i** and **4j** ~ **r** were the incorporation moiety: cinnamic acid and benzoic acid. Generally speaking, coumarin-cinnamic acid derivatives (**4a** ~ **i**) were more active than coumarin-benzoic acid derivatives (**4j** ~ **r**) with the same substitute group. This might due to the potential binding between the cinnamic acid of **4a** ~ **i** and tyrosinase. Furthermore, the substituents in cinnamic acid moiety also had effects on their anti-tyrosinase activity. Compared to compound **4a** with no substituent in cinnamic acid, compounds **4b** ~ **i** showed stronger anti-tyrosinase activity, indicating that the substituent groups including CH_3 , Cl , Br , F , OCH_3 , NO_2 , CF_3 , and OH were benefit for their inhibitory activity.

Coumarin-cinnamic acid derivative **4i** with strongest anti-tyrosinase activity was further structural modified by introduction of various substituents in the coumarin moiety, obtaining derivatives **5a** ~ **l**. Their anti-tyrosinase activity results revealed that the introduction of substituent group (Cl , Br , F , CH_3 , and OCH_3) in the C-6 and C-7 position of coumarin caused a negative effect, however the introduction of hydroxyl would increase their inhibitory activity. Among them, compound **5l** with OH at C-6 position of coumarin showed the best anti-tyrosinase activity (IC_{50} : $3.04 \pm 0.01 \mu\text{M}$), ~ 4.6 folds higher than kojic acid ($14.13 \pm 0.80 \mu\text{M}$).

2.3. Inhibitory mechanism and kinetic type assay

Compound **5l** with the strongest anti-tyrosinase activity was selected as representative molecule to investigate the inhibitory mechanism and kinetic type. The mechanism assay by the plots of v versus $[E]$ in the presence of compound **5l** gave a family of straight lines passing the origin (Fig. 2a), revealing that compound **5l** was a reversible inhibitor. The kinetic type was

detected by Lineweaver-Burk plots of v versus $1/[S]$ in the presence of compound **5l**, that obtained a group of data lines intersecting at \times axis (Fig. 2a). The results showed that compound **5l** showed a noncompetitive inhibition. Moreover, three slope increased with the increasing compound **5l** concentration, and the inhibition constant (K_i) was calculated as $1.5 \mu\text{M}$.

2.4. 3D fluorescence spectra and CD spectra assay

The 3D fluorescence spectra and CD spectra were operated to monitor the tyrosinase conformational changes interacting with compound **5l**. The 3D fluorescence spectra of tyrosinase (Fig. 3a) appeared two typical spectra: Tyr with Trp residues at excitation of 280 nm and emission of 332 nm (Peak 1), and polypeptide backbone structure at excitation of 232 nm and emission of 335 nm (Peak 2). Treatment with compound **5l** ($3.33 \mu\text{M}$) reduced the fluorescence intensity of Peak 1 by 17.87%, and Peak 2 by 28.19% (Fig. 3b), respectively, declaring that the binding of compound **5l** with tyrosinase resulted in the changes of microenvironments and polypeptide backbone structure of tyrosinase.

The CD spectra of tyrosinase with compound **5l** were also monitored at wavelength of 190 ~ 250 nm and shown in Fig. 4. The CD spectra had two negative bands at 210 and 222 nm, those were the typical features of α -helices due to $n \rightarrow \pi^*$ and $\pi \rightarrow \pi^*$ electron transfer of amide. Treatment of compound **5l** caused the visible reduce of negative bands intensity, revealing that binding of compound **5l** with tyrosinase generated the conformation change. The secondary structure contents of tyrosinase in the presence of compound **5l** were calculated and listed in Table 2. Treatment of compound **5l** (molar ratios: 2:1) caused increase in the content of the α -helix (from 7.3 to 9.6%), and β -turn (from 19.8 to 20.6%), while decrease in β -Sheet (from 38.7 to 29.9%) and random coil (from 36.1 to 35.5%).

2.5. Molecular docking

To obtain more binding mode of compound **5l** within the active site of tyrosinase, molecular docking was performed using SYBYL software. As illustrated in Fig. 5(a), compound **5l** was well stabilized into the active site of tyrosinase with a “U shaped” conformation, and 4-hydroxy cinnamic acid moiety nested inside. The detailed interaction results (Fig. 5(b)) showed that 6-hydroxy in coumarin formed a hydrogen bond with His85 (bond length: 1.9 Å), 4-hydroxy in cinnamic acid

Table 1 The anti-tyrosinase activity of all synthetic derivatives **4a** ~ **r** and **5a** ~ **l**.

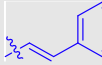
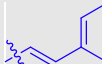
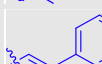

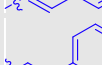

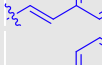
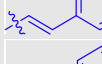
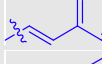
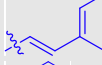
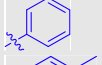
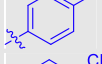
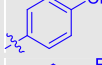
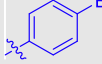
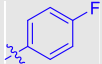
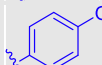
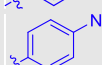
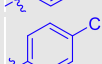
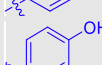
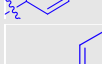
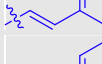
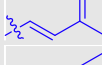
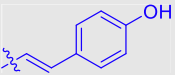
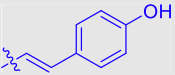
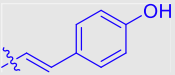
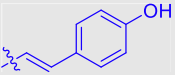
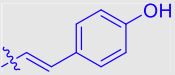
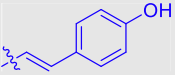
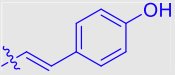
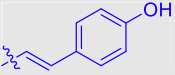
Compound	R ₁	R ₂	R ₃	Inhibition (%) ^a	IC ₅₀ (μM)
4a	H	H		7.48 ± 0.12	–
4b	H	H		44.87 ± 0.17	–
4c	H	H		37.94 ± 0.35	–
4d	H	H		40.32 ± 0.10	–
4e	H	H		30.96 ± 0.14	–
4f	H	H		37.29 ± 0.28	–
4g	H	H		9.62 ± 0.32	–
4h	H	H		27.52 ± 0.30	–
4i	H	H		61.24 ± 0.17	6.40 ± 0.39
4j	H	H		2.45 ± 0.32	–
4k	H	H		9.26 ± 0.21	–
4l	H	H		20.71 ± 0.12	–
4m	H	H		5.17 ± 0.24	–
4n	H	H		7.70 ± 0.14	–
4o	H	H		5.75 ± 0.10	–
4p	H	H		6.08 ± 0.10	–
4q	H	H		5.14 ± 0.20	–
4r	H	H		3.90 ± 0.10	–
5a	Cl	H		26.02 ± 0.30	–
5b	Br	H		35.44 ± 0.21	–
5c	F	H		56.57 ± 0.23	22.91 ± 0.14
5d	CH ₃	H		23.79 ± 0.23	–

Table 1 (continued)

Compound	R ₁	R ₂	R ₃	Inhibition (%) ^a	IC ₅₀ (μM)
5e	OCH ₃	H		60.20 ± 0.23	23.86 ± 0.15
5f	OH	H		62.39 ± 0.17	6.04 ± 0.30
5g	H	Cl		9.43 ± 0.20	–
5h	H	Br		48.55 ± 0.17	44.12 ± 0.36
5i	H	F		53.73 ± 0.30	17.00 ± 0.15
5j	H	CH ₃		58.27 ± 0.40	58.85 ± 0.19
5k	H	OCH ₃		51.31 ± 0.20	52.32 ± 0.67
5l	H	OH		66.24 ± 0.20	3.04 ± 0.01
Kojic acid					14.13 ± 0.80

^a Tyrosinase inhibition was assayed at 64 μM. “–” meant not detected.

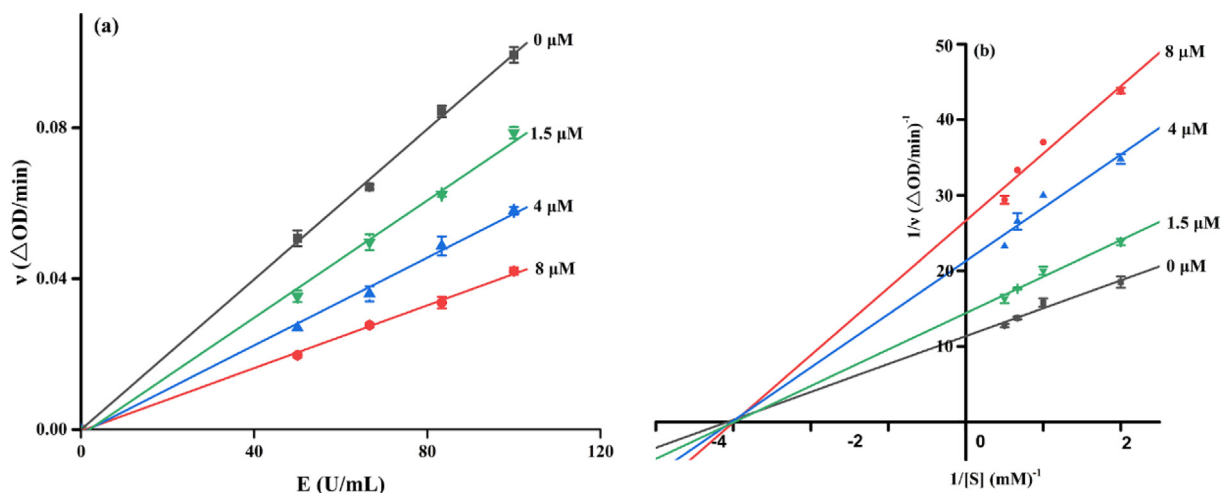


Fig. 2 (a) The plots of v versus $[E]$ in the presence of compound **5l**; (b) Lineweaver-Burk plots of v versus $1/[S]$ in the presence of compound **5l**.

also formed a hydrogen bond with His259 (bond length: 2.7 Å). Moreover, 4-hydroxy in cinnamic acid was oriented toward two Cu ions at distances of 1.9 and 2.8 Å, respectively. All interactions helped compound **5l** to anchor into the active site of tyrosinase.

2.6. Melanogenesis and tyrosinase activity assay in B16F10 cells

The cytotoxicity of representative compound **5l** on B16F10 cells was firstly assayed after treatment of compound **5l** for 48 h (Fig. 6). The results verified that compound **5l** had no tox-

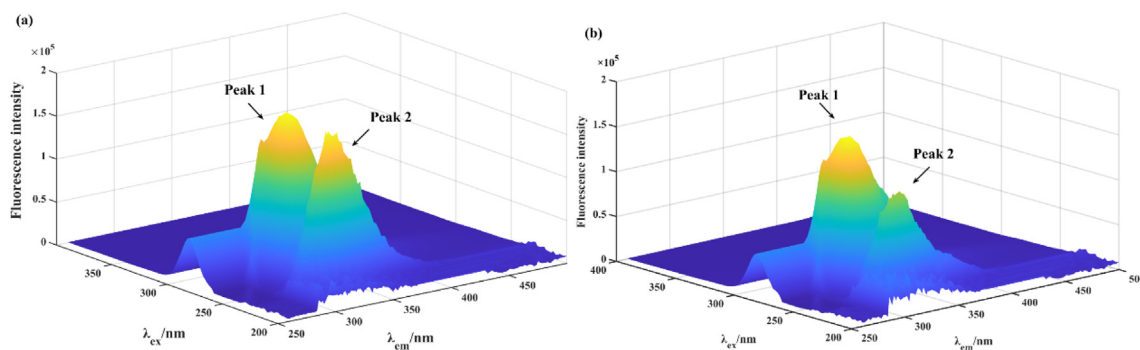


Fig. 3 (a) The 3D fluorescence spectra of tyrosinase. (b) The 3D fluorescence spectra of tyrosinase with compound **5I**.

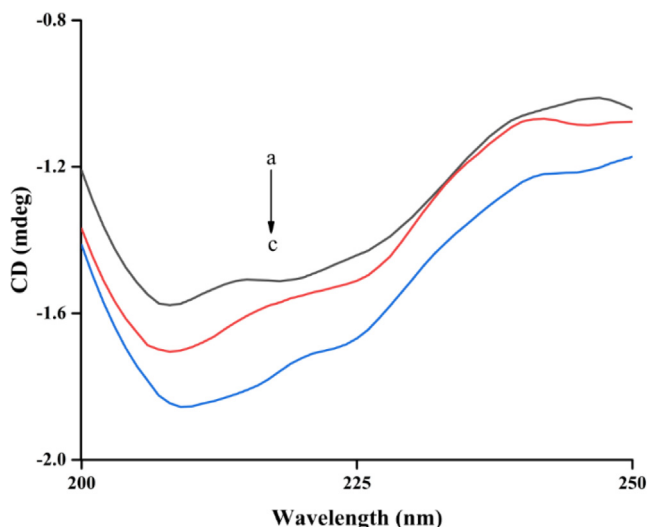


Fig. 4 The CD spectra of tyrosinase and compound **5I** complex. The molar ratios of tyrosinase to **5I** were 1: 0, 1: 1, and 1: 2 for curves a-c, respectively.

icity effect on B16F10 cells up to concentration 32 μM , while compound **5I** showed obvious cytotoxicity at 64 μM . On the other hand, kojic acid (8–64 μM) showed no cytotoxicity. Therefore, the effects of compound **5I** on melanogenesis and tyrosinase activity *in vitro* were performed at concentrations (8–32 μM) with no cytotoxicity on B16F10 cells.

The inhibitory effects of compound **5I** on melanogenesis were ascertained by measuring the melanin content of B16F10 cells that were treated with compound **5I** (8–32 μM)

for 48 h. As can be seen in Fig. 7, compound **5I** (8–32 μM) presented effectively melanin inhibition in a dose-dependent manner, showing ($9.69 \pm 1.69\%$), ($16.41 \pm 1.15\%$), and ($20.96 \pm 1.62\%$), respectively. Moreover, compound **5I** existed stronger melanin inhibitory activity than kojic acid at same tested concentrations.

The cellular tyrosinase inhibitory effects of compound **5I** were also determined in B16F10 cells and the results were listed in Fig. 8. Compound **5I** (8–32 μM) exerted markedly inhibitory activity on cellular tyrosinase in a dose-dependent manner, with inhibition rate of ($17.94 \pm 2.06\%$), ($21.77 \pm 1.17\%$), and ($32.30 \pm 1.47\%$), respectively, which were higher than those of kojic acid, respectively. Those results established that compound **5I** suppressed melanogenesis by the inhibition of tyrosinase.

2.7. Melanogenesis and tyrosinase activity assay in zebrafish

To address whether the depigment effects of compound **5I** also occurs *in vivo*, we employed zebrafish model that had been believed as the typical *in vivo* model for the evaluation of tyrosinase activity and melanin. The acute toxicity of compound **5I** was firstly evaluated. Fish embryos were exposed to compound **5I** for 48 h to observe the embryo survival. The survival rate of compound **5I** and kojic acid ranged from 85% to 95% (Fig. 9), revealing that compound **5I** and kojic acid did not show acute toxicity at the tested concentrations (10–160 μM).

Then, the effects of compound **5I** (10–40 μM) on melanogenesis in zebrafish were assayed by analyzing the grayscale value of the photo of embryo (Fig. 10). The results indicated that fish embryos in control group presented obvious pigmen-

Table 2 The secondary structures contents of tyrosinase-compound **5I** complex.

[Tyrosinase]: [Compound 5I]	α -Helix (%)	β -Sheet (%)	β -Turn (%)	Rndm Coil (%)
1:0	7.3	38.7	19.8	36.1
1:1	7.8	36.5	20	35.9
1:2	9.6	29.9	20.6	35.5

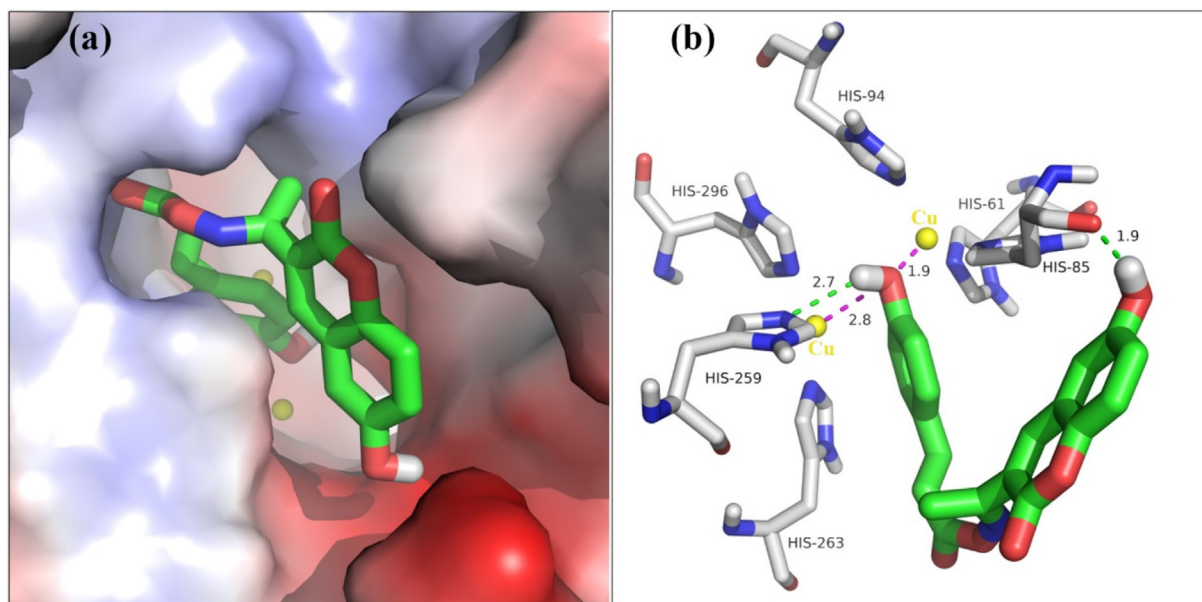


Fig. 5 (a) Compound 5I is positioned into the active pocket. (b) Detailed interaction of compound 5I with tyrosinase.

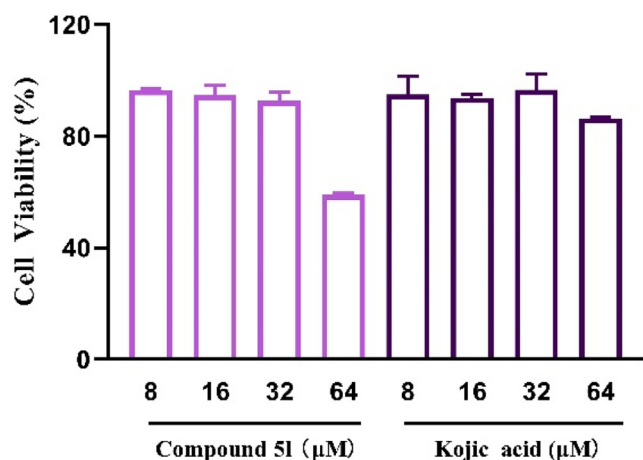


Fig. 6 The cytotoxicity assay of compound 5I and kojic acid in B16F10 cells.

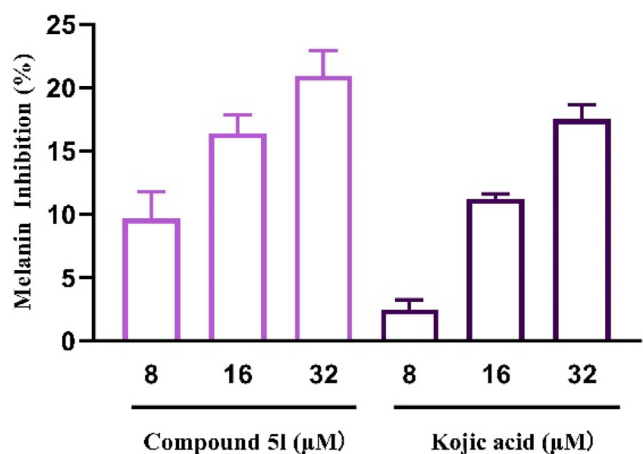


Fig. 7 The melanin inhibition of compound 5I and kojic acid in B16F10 cells.

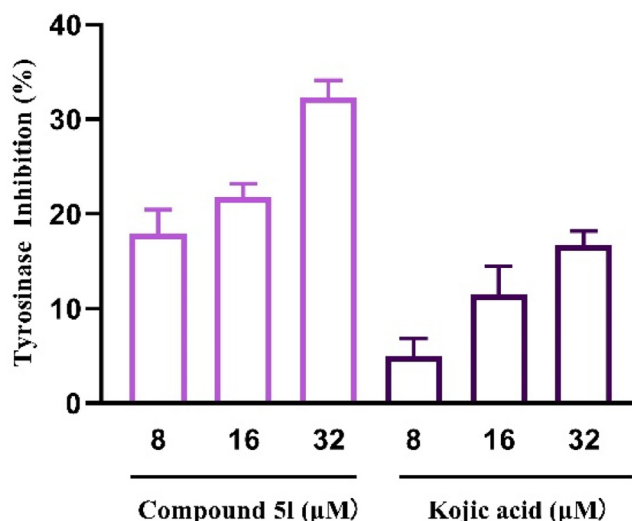


Fig. 8 The cellular tyrosinase inhibitory of compound 5I and kojic acid in B16F10 cells.

tation, especially in the eyes, yolk sac and notum. However, treatment with compound 5I (10–40 μM) could effectively reduce the pigmentation in a dose-dependent manner to (30 ± 5)%, while kojic acid showed (23 ± 3)% at 40 μM. Additionally, compound 5I (10–20 μM) exhibited better depigmenting effects, relative to kojic acid.

The effects of compound 5I (10–40 μM) on tyrosinase activity in zebrafish were finally detected and the results were shown in Fig. 11. Compound 5I effectively inhibited tyrosinase activity in zebrafish in a dose-dependent manner to (57.03 ± 2.19)% at 40 μM, which was slightly lower than that of kojic acid (63.09 ± 3.82)% at 40 μM. Additionally, compound 5I (10–20 μM) exhibited better anti-tyrosinase activity than kojic acid at the same concentrations. This linear reduction of melanogenesis and tyrosinase activity in zebrafish embryos matched

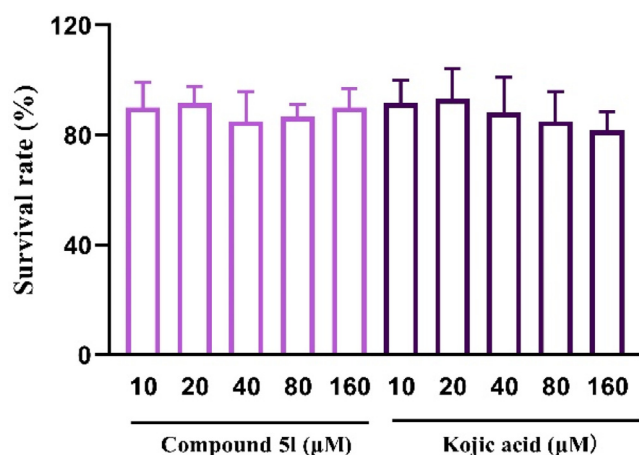


Fig. 9 The acute toxicity assay of compound **5I** and kojic acid in zebrafish.

that obtained in the B16 cell, revealing the positive *in vitro-in vivo* correlation.

3. Conclusion

In order to develop potent tyrosinase inhibitors, we designed and synthesized hybrids (**4a** ~ **r**, **5a** ~ **l**) coumarin and cinnamic acid/benzoic

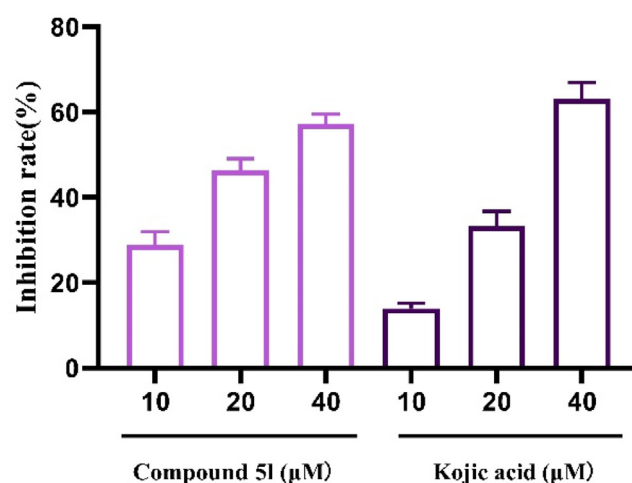


Fig. 11 The tyrosinase inhibitory of compound **5I** and kojic acid in zebrafish.

acid constituted by coumarin and cinnamic acid/benzoic acid through oxime linkage. Among them, compound **5I** exhibited outstanding anti-tyrosinase activity with IC_{50} of $3.04 \pm 0.01 \mu\text{M}$ compared to $14.13 \pm 0.80 \mu\text{M}$ of kojic acid. Kinetic study revealed compound **5I** to be a reversible and uncompetitive tyrosinase inhibitor. 3D fluorescence and CD spectra results showed treatment of compound **5I** lead to

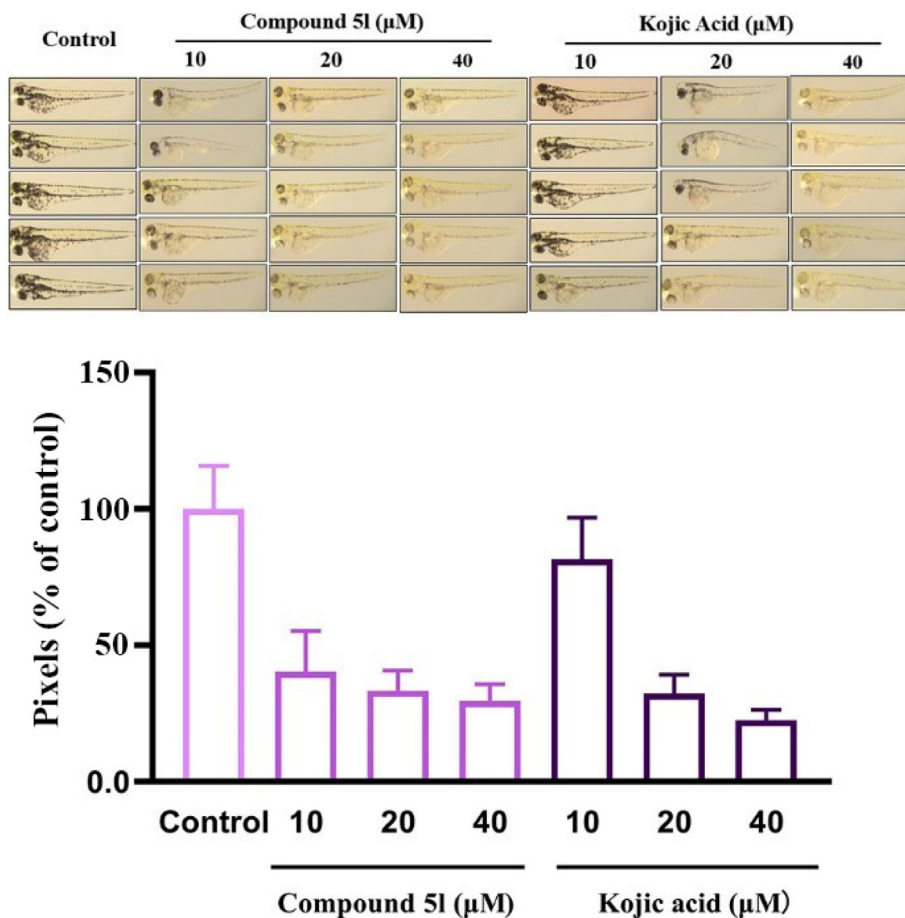


Fig. 10 The melanin inhibition of compound **5I** and kojic acid in zebrafish.

the conformational changes of tyrosinase. Molecular docking revealed the binding between compound **5I** and tyrosinase. Furthermore, compound **5I** inhibited melanin content and cellular tyrosinase activity both in B16F10 cells and zebrafish model with no toxicity effect. Taken together, our findings suggested that compound **5I** could be used as potential candidate to relieve tyrosinase-related hyperpigmentation. All studies highlight the importance of coumarin derivatives as promising anti-melanin agents and provided a method for developing this inhibitors.

4. Experimental

4.1. Materials and methods

Tyrosinase from mushroom (EC 1.14.18.1) and 3,4-Dihydroxyphenylalanine (L-DOPA) were purchased from Sigma-Aldrich. All other reagents and solvents were commercial available. ^1H NMR and ^{13}C NMR spectra were recorded in CDCl_3 on 500 MHz instruments. High-resolution mass spectral analysis (HRMS) data were measured on the Apex II by means of the ESI technique.

4.2. Synthesis of derivatives **4a** ~ **r** and **5a** ~ **l**

Substituted salicylaldehyde (**1**) (1.0 mmol) and ethyl acetoacetate (1.1 mmol) were added into 10 mL of ethanol containing piperidine (0.02 mmol), then refluxed at 80 °C until the reaction completed. Ice-cold water was added to quench the reaction, followed by filtration and recrystallization to obtain substituted acetyl coumarin (**2**). To the solution of **2** (1.0 mmol) in 10 mL of ethanol, hydroxylamine hydrochloride (3.0 mmol) and pyridine (0.04 mmol) were added and reacted at room temperature. The product was washed with ethanol to obtain substituted acetyl coumarin containing oxime (**3**). To the solution of **3** (1.0 mmol) in 3 mL of DCM, triethylamine (1.1 mmol) and substituted benzoic acid chlorides/cinnamic acid chlorides (1.0 mmol) were added, respectively, and reacted at room temperature. Then the reaction was quenched, extracted, washed, and dried, followed by column chromatography purification to produce derivatives **4a** ~ **r** and **5a** ~ **l**. All NMR, HRMS, yield, and m.p. data were summarized in [supplementary material](#).

4.3. Tyrosinase activity assay

The synthetic derivatives were assayed for anti-tyrosinase activity using mushroom tyrosinase and L-DOPA (He et al., 2021; Song et al., 2017). All derivatives were dissolved in DMSO and diluted to various concentrations. 10 μL of mushroom tyrosinase (1333.4 U/mL) and 10 μL of test compound were added into 130 μL of phosphate buffer (50 M, pH 6.8), respectively, followed by the incubation for 10 min at room temperature. Then 50 μL of L-DOPA solution (2 mM) was added and the absorbance change was determined at 475 nm. The inhibition percentage was calculated respect to blank group and the 50% inhibitory concentration (IC_{50}) was calculated by interpolation of the dose–response curves. Kojic acid was used as the positive standard. Each experiment was done four times in parallel.

The enzyme inhibitory kinetics of compound **5I** were determined by the plots of enzymatic reaction vs enzyme concentra-

tion in the presence of compound **5I** (Hu et al., 2016), and the substrate inhibitory kinetics were obtained by the Lineweaver-Burk plot of enzymatic reaction vs substrate concentration in the presence of compound **5I** (Zhao et al., 2019). The final L-DOPA concentrations were 0.5, 1, 0.67, and 2, respectively.

4.4. 3D fluorescence spectra assay

10 μL of mushroom tyrosinase (Final concentration: 168 μM) and 10 μL of compound **5I** (Final concentration: 3.33 μM) were added into 2.98 mL of phosphate buffer (50 M, pH 6.8) and incubated for 5 min (Song et al., 2020). The 3D fluorescence spectra of this mixture were measured at excitation and emission wavelengths of 200–600 nm.

4.5. CD spectroscopy

10 μL of mushroom tyrosinase (Final concentration: 33 μM) and 10 μL of compound **5I** were added into 180 μL of phosphate buffer (50 M, pH 6.8) and incubated for 5 min (Song et al., 2021). The CD spectrum of this mixture was recorded. The proportion of secondary conformation of protein was analyzed using CDNN.

4.6. Molecular docking

Molecular docking was performed by SYBYL software using the crystal structure of tyrosinase from *Agaricus bisporus* (PDBID: 2Y9X) obtained from the RCSB Protein Data Bank (Peng et al., 2021). The tyrosinase protein was prepared by the remove of ligand and water, followed by the addition of hydrogen atoms and charge, repair of end residues, and the generation of active pocket. Compound **5I** was prepared by addition of charge with Gasteiger-Hückle and energy minimization. Then, the docking between Compound **5I** and tyrosinase was operated in the default format, and the results were visualized by Pymol software.

4.7. Cell culture

B16F10 cells (ATCC, Manassas, VA, USA) were cultured in DMEM supplemented with 10% FBS and 1% penicillin/streptomycin at 37 °C in a humidified atmosphere with 5% CO_2 .

4.8. Cytotoxicity assay

The cells viability after exposure to compound was determined by MTT method as described previously (Lee et al., 2019). B16F10 cells were seeded in a 96 well plate (5×10^3 cells/well) for 24 h and treated with compound **25** (10–40 μM) for another 24 h. Then cells were labelled with MTT solution (0.5 mg/mL) for 4 h. The violet formazan precipitates were dissolved in 100 μL DMSO, then the absorbance was measured at 570 nm. Kojic acid was used as a positive control.

4.9. Melanin assay in B16F10 cells

The effect of compound **5I** on melanin content was studied in Murine B16F10 melanoma cells using the standard method with slight modification (Ullah et al., 2019). B16F10 cells were

seeded in a 6 well plate (10^5 cells/well) for 24 h, and then treated with compound **51** ($8 \sim 32 \mu\text{M}$) for another 48 h. Harvested cells were added 200 μL NaOH (1 M, containing 10% DMSO), heated at 100°C for 1 h, and then the absorbance at 405 nm was detected. Kojic acid ($8 \sim 32 \mu\text{M}$) was used as a positive control.

4.10. Tyrosinase activity in B16F10 cells

The cellular tyrosinase inhibition of compound **51** was performed as previously described with slight modification (Tang et al., 2021). B16F10 cells were seeded in a 6 well plate (10^5 cells/well) for 24 h, and then treated with compound **51** ($8 \sim 32 \mu\text{M}$) for 48 h. Harvested cells were washed with ice-cold PBS two times, added 300 μL Triton X-100 (1%, 50 mM PBS), and frozen at -80°C for 1 h. Then cellular extracts were thawed and centrifuged (12000 rpm, 4°C) for 30 min to obtain the supernatant, followed by the protein concentration determination using BCAKit. To 80 μL protein solution (equal amount of protein), 20 μL of L-DOPA solution (10 mM) was added, and then the absorbance change was determined at 475 nm. Kojic acid ($8 \sim 32 \mu\text{M}$) was used as a positive control.

4.11. Zebrafish maintenance

Sexual maturity, health, and no deformity Wild-type (AB) zebrafish were cultured at 28°C under a 14/10-hr light/dark cycle with the pH around 7.4.

4.12. Fish embryo acute toxicity test

For the *in vivo* toxicity test (Ramlan et al., 2017); 6 \sim 8 hpf embryos were seeded in 24 well plate with M3 culture medium (1 embryo/well), treated with test compound ($0 \sim 160 \mu\text{M}$) and Kojic acid ($0 \sim 160 \mu\text{M}$), respectively, then observed the survival at 72 hpf. Kojic acid ($0 \sim 160 \mu\text{M}$) was used as a positive control. Each condition had 12 embryos and was repeated 5 times.

4.13. Melanin determination in zebrafish

Phenotype-based melanogenesis inhibition of compound **51** in zebrafish was determined following reported method (Abbas et al., 2017). Embryos were seeded in 6 well plate with M3 culture medium (5 embryo/well) at 24 hpf, treated with test compound ($0 \sim 40 \mu\text{M}$) and Kojic acid ($0 \sim 40 \mu\text{M}$), respectively. Then the photo of embryo was taken to determine the melanin using image J software. The embryo photo was prepared with built-in program of image J software, including converging picture to grayscale, framing embryo photo, closing resulting curve, reading grayscale. The grayscale of sample embryo photo was expressed as relative melanin level of the control (100%).

4.14. Tyrosinase activity in zebrafish

Tyrosinase activity was measured according to the method by Chen et al. (Chen et al., 2019). The treated embryos were lysed in 150 μL sodium deoxycholate solution (5.0 mg/mL),

and centrifuged (10000 rpm, 4°C) for 5 min to obtain the supernatant. 100 μL supernatant was mixed with 100 μL L-DOPA solution (5 mg/mL), followed by the absorbance change record at 475 nm.

4.15. Statistical analysis

All data were presented as mean \pm SD. One-way ANOVA was performed to evaluate the difference between groups. $P < 0.05$ was considered significant.

Declaration of Competing Interest

The authors declare that they have no known competing financial interests or personal relationships that could have appeared to influence the work reported in this paper.

Acknowledgements

This work was financially supported by the Fundamental and Applied Basic Research Fund of Guangdong Province (No. 2022A1515011657), Department of Education of Guangdong Province (Nos. 2019KZDXM035, 2021KTSCX135, 2021KCXTD044), Jiangmen Science and Technology Plan Project (2021030103150006664), Joint research fund for Wuyi university and Hong Kong and Macao (2021WGALH08), the Science and Technology Development Fund, Macau SAR (0043/2020/AGJ) and the Department of Science and Technology of Guangdong Province for the support of Guangdong-Hong Kong-Macao Joint Laboratory of Respiratory Infectious Disease.

Appendix A. Supplementary material

Supplementary data to this article can be found online at <https://doi.org/10.1016/j.arabjc.2023.104724>.

References

- Abbas, Q., Ashraf, Z., Hassan, M., Nadeem, H., Latif, M., Afzal, S., Seo, S.Y., 2017. Development of highly potent melanogenesis inhibitor by *in vitro*, *in vivo* and computational studies. *Drug Des. Dev. Ther.* 11, 2029.
- Ashooriha, M., Khoshneviszadeh, M., Khoshneviszadeh, M., Rafiei, A., Kardan, M., Yazdian-Robati, R., Emami, S., 2020. Kojic acidenatural product conjugates as mushroom tyrosinase inhibitors. *Eur. J. Med. Chem.* 201, 112480.
- Ashraf, Z., Rafiq, M., Seo, S.Y., Kwon, K.S., Babar, M.M., Zaidi, N. S., 2015. Kinetic and *in silico* studies of novel hydroxy-based thymol analogues as inhibitors of mushroom tyrosinase. *Eur. J. Med. Chem.* 98, 203–211.
- Ashraf, Z., Rafiq, M., Seo, S.Y., Babar, M.M., Zaidi, N.S., 2015. Design, synthesis and bioevaluation of novel umbelliferone analogues as potential mushroom tyrosinase inhibitors. *J. Enzyme Inhib. Med. Chem.* 30, 874–883.
- Asthana, S., Zucca, P., Vargiu, A.V., Sanjust, E., Ruggerone, P., Rescigno, A., 2015. Structure-activity relationship study of hydroxycoumarins and mushroom tyrosinase. *J. Agric. Food Chem.* 63, 7236–7244.
- Chen, Y.M., Su, W.C., Li, C., Shi, Y., Chen, Q.X., Zheng, J., Tang, D. L., Chen, S.M., Wang, Q., 2019. Anti-melanogenesis of novel kojic acid derivatives in B16F10 cells and zebrafish. *Int. J. Biol. Macromol.* 123, 723–731.

- Fu, D., Yuan, Y., Qin, F., Xu, Y., Cui, X., Li, G., Yao, S., Deng, Y., Tang, Z., 2021. Design, synthesis and biological evaluation of tyrosinase-targeting PROTACs. *Eur. J. Med. Chem.* 226, 113850.
- He, M., Fan, M., Liu, W.J., Li, Y.J., Wang, G.C., 2021. Design, synthesis, molecular modeling, and biological evaluation of novel kojic acid derivatives containing bioactive heterocycle moiety as inhibitors of tyrosinase and antibrowning agents. *Food Chem.* 362, 130241.
- Hu, Y.H., Chen, Q.X., Cui, Y., Gao, H.J., Xu, L., Yu, X.Y., Wang, Y., Yan, C.L., Wang, Q., 2016. 4-Hydroxy cinnamic acid as mushroom preservation: anti-tyrosinase activity kinetics and application. *Int. J. Biol. Macromol.* 86, 489–495.
- Imokawa, G., Nakajima, H., Ishida, K., 2015. Biological mechanisms underlying the ultraviolet radiation-induced formation of skin wrinkling and sagging II: overexpression of neprilysin plays an essential role. *Int. J. Mol. Sci.* 16, 7776–7795.
- Jitareanu, A., Pădureanu, S., Tătăringă, G., Tuchilus, C., Stănescu, U., 2013. Evaluation of phytotoxic and mutagenic effects of some cinnamic acid derivatives using the *Triticum* test. *Turk. J. Biol.* 37, 748–756.
- Kong, Y.H., Jo, Y.O., Cho, C.W., Son, D., Park, S., Rho, J., Choi, S. Y., 2008. Inhibitory effects of cinnamic acid on melanin biosynthesis in skin. *Biol. Pharm. Bull.* 31, 946–954.
- Kostova, I., 2005. Synthetic and natural coumarins as cytotoxic agents. *Curr. Med. Chem. Anti Cancer Agents* 5, 29–46.
- Lee, S., Ullah, S., Park, C., Lee, H.W., Kang, D.W., Yang, J., Akter, J., Park, Y.J., Chun, P., Moon, H.R., 2019. Inhibitory effects of N-(acryloyl)benzamide derivatives on tyrosinase and melanogenesis. *Bioorg. Med. Chem.* 27, 3929–3937.
- Li, J., Feng, L., Liu, L., Wang, F., Ouyang, L., Zhang, L., Hu, X., Wang, G., 2021. Recent advances in the design and discovery of synthetic tyrosinase inhibitors. *Eur. J. Med. Chem.* 224, 113744.
- Lin, J.Y., Fisher, D.E., 2007. Melanocyte biology and skin pigmentation. *Nature* 445, 843–850.
- Liu, J., Wu, F.Y., Chen, L.J., Zhao, L.Z., Zhao, Z.B., Wang, M., Lei, S., 2012. Biological evaluation of coumarin derivatives as mushroom tyrosinase inhibitors. *Food Chem.* 135, 2872–2878.
- Matos, M.J., Santana, L., Uriarte, E., Delogu, G., Corda, M., Fadda, M.B., Era, B., Fais, A., 2011. New halogenated phenylcoumarins as tyrosinase inhibitors. *Bioorg. Med. Chem. Lett.* 21, 3342–3345.
- Matos, M.J., Varela, C., Vilar, S., Hripcsak, G., Borges, F., Santana, L., Uriarte, E., Fais, A., Di Petrillo, A., Pintus, F., Era, B., 2015. Design and discovery of tyrosinase inhibitors based on a coumarin scaffold. *RSC Adv.* 5, 94227.
- Moreiras, H., Pereira, F.J.C., Neto, M.V., Seabra, M.C., Barral, D.C., 2020. The exocyst is required for melanin exocytosis from melanocytes and transfer to keratinocytes. *Pigm. Cell. Melanoma.* R. 33, 366–371.
- Musa, M.A., Cooperwood, J.S., 2008. A review of coumarin derivatives in pharmacotherapy of breast cancer. *Curr. Med. Chem.* 15, 2664–2679.
- Pang, G.X., Niu, C., Mamat, N., Aisa, H.A., 2017. Synthesis and in vitro biological evaluation of novel coumarin derivatives containing isoxazole moieties on melanin synthesis in B16 cells and inhibition on bacteria. *Bioorg. Med. Chem. Lett.* 27, 2674–2677.
- Parvez, S., Kang, M., Chung, H.-S., Bae, H., 2007. Naturally occurring tyrosinase inhibitors: mechanism and applications in skin health, cosmetics and agriculture industries. *Phytother. Res.* 21, 805–816.
- Peng, Z.Y., Wang, G.C., Zeng, Q.H., Li, Y.F., Wu, Y., Liu, H.Q., Wang, J.J., Zhao, Y., 2021. Synthesis, antioxidant and anti-tyrosinase activity of 1,2,4-triazole hydrazones as antibrowning agents. *Food Chem.* 341, 128265.
- Pillaiyar, T., Namasivayam, V., Manickam, M., Jung, S.H., 2018. Inhibitors of melanogenesis: an updated review. *J. Med. Chem.* 61, 7395–7418.
- Radhakrishnan, S.K., Shimmon, R.G., Conn, C., Baker, A.T., 2016. Evaluation of novel chalcone oximes as inhibitors of tyrosinase and melanin formation in B16 cells. *Arch. Pharm. Chem. Life Sci.* 349, 20–29.
- Ramlan, N.F., Sata, N.S.A.M., Hassan, S.N., Bakar, N.A., Ahmad, S., Zulkifli, S.Z., Abdullah, C.A.C., Ibrahim, W.N.W., 2017. Time dependent effect of chronic embryonic exposure to ethanol on zebrafish: Morphology, biochemical and anxiety alterations. *Behav. Brain Res.* 332, 40–49.
- Roberts, N.B., Curtis, S.A., Milan, A.M., Ranganath, L.R., 2015. The pigment in alkaptonuria relationship to melanin and other coloured substances: a review of metabolism, composition and chemical analysis. *JIMD Rep.* 24, 51–66.
- Romagnoli, R., Oliva, P., Prencipe, F., Manfredini, S., German, M.P., De Luca, L., Ricci, F., Corallo, D., Aveic, S., Mariotto, E., Viola, G., Bortolozzi, R., 2022. Cinnamic acid derivatives linked to arylpiperazines as novel potent inhibitors of tyrosinase activity and melanin synthesis. *Eur. J. Med. Chem.* 231, 114147.
- Sánchez-Ferrer, Á., Neptuno Rodríguez-López, J., García-Cánovas, F., García-Carmona, F., 1995. Tyrosinase: a comprehensive review of its mechanism. *Biochim. Biophys. Acta* 1247, 1–11.
- Shao, L.L., Wang, X.L., Chen, K., Dong, X.W., Kong, L.M., Zhao, D.Y., Hider, R.C., Zhou, T., 2018. Novel hydroxypyridinone derivatives containing an oxime ether moiety: synthesis, inhibition on mushroom tyrosinase and application in antibrowning of fresh-cut apples. *Food Chem.* 242, 174–181.
- Sheng, Z., Ge, S., Xu, X., Zhang, Y., Wu, P., Zhang, K., Xu, X., Li, C., Zhao, D., Tang, X., 2018. Design, synthesis and evaluation of cinnamic acid ester derivatives as mushroom tyrosinase inhibitors. *Medchemcomm* 9, 853–861.
- Song, X., Hu, X., Zhang, Y., Pan, J.H., Gong, D.M., Zhang, G.W., 2020. Inhibitory mechanism of epicatechin gallate on tyrosinase: inhibitory interaction, conformational change and computational simulation. *Food Funct.* 11, 4892–4902.
- Song, X., Ni, M.T., Zhang, Y., Zhang, G.W., Pan, J.H., Gong, D.M., 2021. Comparing the inhibitory abilities of epigallocatechin-3-gallate and gallic acid against tyrosinase and their combined effects with kojic acid. *Food Chem.* 349, 129172.
- Song, S.C., You, A., Chen, Z.Y., Zhu, G.X., Wen, H., Song, H.C., Yi, W., 2017. Study on the design, synthesis and structure-activity relationships of new thiosemicarbazone compounds as tyrosinase inhibitors. *Eur. J. Med. Chem.* 139, 815–825.
- Tang, K., Jiang, Y., Zhang, H., Huang, W.L., Xie, Y.D., Deng, C., Xu, H.B., Song, X.M., Xu, H., 2021. Design, synthesis of Cinnamyl-paeonol derivatives with 1, 3-Dioxypropyl as link arm and screening of tyrosinase inhibition activity in vitro. *Bioorg. Chem.* 106, 104512.
- Taofiq, O., González-Paramás, A., Barreiro, M.F., Ferreira, I.C., 2017. Hydroxycinnamic acids and their derivatives: cosmeceutical significance, challenges and future perspectives, a review. *Molecules* 22, 281–304.
- Ullah, S., Park, Y., Ikram, M., Lee, S., Park, C., Kang, D., Yang, J., Akter, J., Yoon, S., Chun, P., Moon, H.R., 2018. Design, synthesis and anti-melanogenic effect of cinnamide derivatives. *Bioorg. Med. Chem.* 26, 5672–5681.
- Ullah, S., Kang, D., Lee, S., Ikram, M., Park, C., Park, Y., Yoon, S., Chun, P., Moon, H.R., 2019. Synthesis of cinnamic amide derivatives and their anti-melanogenic effect in alpha-MSH-stimulated B16F10 melanoma cells. *Eur. J. Med. Chem.* 161, 78–92.
- Ullah, S., Park, C., Ikram, M., Kang, D., Lee, S., Yanga, J., Park, Y. J., Yoon, S., Chun, P., Moon, H.R., 2019. Tyrosinase inhibition and anti-melanin generation effect of cinnamide analogue. *Bioorg. Chem.* 87, 43–55.
- Xu, X.T., Deng, X.Y., Chen, J., Liang, Q.M., Zhang, K., Li, D.L., Wu, P.P., Zheng, X., Zhou, R.P., Jiang, Z.Y., Ma, A.J., Chen, W. H., Wang, S.H., 2020. Synthesis and biological evaluation of coumarin derivatives as α -glucosidase inhibitors. *Eur. J. Med. Chem.* 189, 112013.

- Xu, F., Zhang, S.H., Shao, R.G., Zhen, Y.S., 2005. Anticancer activity of sodium caffeate and its mechanism. *Acta Pharmacol. Sin.* 26, 1248–1252.
- Yuan, Y., Jin, W., Nazir, Y., Fercher, C., Blaskovich, M.A.T., Cooper, M.A., Barnard, R.T., Ziora, Z.M., 2020. Tyrosinase inhibitors as potential antibacterial agents. *Eur. J. Med. Chem.* 187, 111892.
- Zhao, Z.F., Liu, G.X., Meng, Y.F., Tian, J.L., Chen, X.F., Shen, M. L., Li, Y.X., Li, B.Y., Gao, C., Wu, S.P., Li, C.Q., He, X.R., Jiang, R., Qian, M.C., Zheng, X.H., 2019. Synthesis and anti-tyrosinase mechanism of the substituted vanillyl cinnamate analogues. *Bioorg. Chem.* 93, 103316.
- Zolghadri, S., Bahrami, A., Hassan Khan, M.T., Munoz-Munoz, J., Garcia-Molina, F., Garcia-Canovas, F., Saboury, A.A., 2019. A comprehensive review on tyrosinase inhibitors, *J. Enzym. Inhib. Med. Chem.* 34, 279–309.